PHYSICAL REVIEW E VOLUME 51, NUMBER 1 JANUARY 1995

Properties of wave functions in homogeneous anisotropic media

Wei Ren
China Center of Advanced Science and Technology (World Laboratory), P.O. Box 8730, Beijing 100080, People's Republic of China and Department of Applied Mathematics, University of Electronic Science and Technology of China, Chengdu, Sichuan 610054, People's Republic of China

Xin Bao Wu
China Research Institute of Radiowave Propagation, P.O. Box 138, Xinxiang, Henan 453003, People's Republic of China

Zhang Yi
Institute of Mathematics, Academia Sinica, Beijing 100080, People's Republic of China and Department of Applied Mathematics, University of Electronic Science and Technology of China, Chengdu, Sichuan 610054, People's Republic of China

Wei Gan Lin
University of Electronic Science and Technology of China, Chengdu, Sichuan 610054, People's Republic of China

(Received 8 March 1994)

The general solutions of the first, second, third, and fourth kinds to the wave equation in homogeneous anisotropic media are expressed by integrals over a finite range. The convergence of the series solution of wave functions in homogeneous anisotropic media [Phys. Rev. E **47**, 664 (1993)] is discussed. The use of the wave functions in anisotropic media is demonstrated. The theory is expounded via an illustrative example of a two-dimensional scalar case. The analytical solution of plane-wave scattering by a conducting circular cylinder coated with anisotropic materials is formulated in terms of the series of wave functions for anisotropic media. Numerical results show that the solution in terms of wave functions of various kinds in anisotropic media gives essentially the same radar cross sections as obtained by Beker, Umashankar, and Taflove [Electromagnetics **10**, 387 (1990)] using a different approach. Numerical results in the resonance region are presented for reference purposes. The analysis of this paper can be easily generalized to vector and tensor wave functions in homogeneous anisotropic media.

PACS number(s): 42.25.Bs, 03.40.Kf

I. INTRODUCTION

The scattering by anisotropic objects has attracted a great deal of interest [1–12]. Among them, one should mention the scattering by a perfect conducting cylinder covered with anisotropic layers [1], and the exact solutions to wave equations in cylindrically homogeneous (i.e., in a circular cylindrical coordinate system, the tensor elements of the anisotropic media are constant) anisotropic media [2]. (In this paper, we deal with the waves in a *Cartesian homogeneous* anisotropic medium, i.e., in a rectangular coordinate system, the anisotropic medium tensors are constants. Work beyond the medium of this kind will not be mentioned further.) In addition, one should mention the moment method solutions to the Cartesian homogeneous anisotropic media [3], the variational reaction formulation [4], the plane-wave angular spectrum method based on the integral equation [5,6], the boundary integral equation solvers for two-dimensional cylindrical structures [7–9], the coupled dipole method [10], the integral equation techniques [11], and the frequency domain finite difference method [12].

In a series of papers [13–15], Ren has developed a method to solve the homogeneous and inhomogeneous wave equations in homogeneous anisotropic media. The series representations of the wave functions of the first, second, third, and fourth kinds for homogeneous anisotropic media are obtained. Since the general dispersion equation for the homogeneous bianisotropic media is available now [16], the extension of the wave-function theory to bianisotropic media becomes straightforward. Moreover, there are similarities between the Ren solution [13–15] and the classical wave-function theory for isotropic media [17]. Recently, the series solution to the scattering by an anisotropic circular cylinder is formulated by the wave functions in anisotropic media [18]; and the numerical results of Ref. [18] show an excellent agreement between the solution based on the scalar circular wave functions of the first kind and other solutions using different methods. The solution is formally similar to the elliptic cylinder wave-function solution to the scattering by an isotropic elliptic cylinder.

In this article, two essential features of Ren's previous articles [13–15] are followed. One is the art of transforming the eigen plane waves in the unbounded anisotropic media into the wave functions suitable for applications to bounded geometries. Another is the key method of developing the wave-function theory in anisotropic media by means of the well known wave-function theory in isotropic media. Our method is expounded by the

1063-651X/95/51(1)/671(9)/$06.00

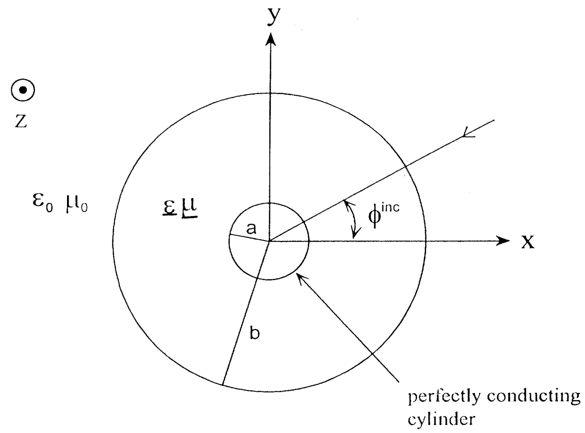

FIG. 1. Geometry of the problem.

two-dimensional scalar wave functions in homogeneous anisotropic media. The angular spectrum representations of the fields inside a circle of homogeneous anisotropic media, proved in many papers [5–8, 11–13], are taken as the starting point of our theory.

The plan of this paper is as follows. In Sec. II, we first give the general solution of various kinds to the nonstandard wave equation in anisotropic media by a finite range of integrals, which is easily proven to be a solution to the nonstandard wave equation. We further prove that these integral representations do include all the solutions of the nonstandard wave equation. Namely, no solution is lost. Such a proof is completed by using the well known existing results on solutions to the standard wave equation in isotropic media. Second, we show that in the anisotropic media the series solution, in terms of wave functions of various kinds, is convergent to the general solutions of corresponding kind. Third, we show how to formulate the boundary value problems in terms of the wave functions of various kinds in anisotropic media via the illustrative example shown in Fig. 1. The similarities of the solutions between a conducting circular cylinder coated with anisotroipic materials and an isotropic dielectric-coated elliptic cylinder [19,20] are revealed. Numerical verification and implementation are given in Sec. III. Numerical results in the low frequency range are presented for the purpose of numerical validation. The agreement is excellent. Numerical results in the resonance range are also presented to show the numerical efficiency of our method, and to provide references for future computations using other methods by other authors. Section IV concludes this article with a discussion of relevant problems.

In the expressions for the electromagnetic fields, the time dependence $\exp(j\omega t)$ is assumed and suppressed.

II. THEORY

Consider a homogeneous anisotropic medium characterized by the following permittivity and permeability tensors:

$$\underline{\varepsilon}=\begin{bmatrix}\varepsilon_{xx} & \varepsilon_{xy} & 0\\ \varepsilon_{yx} & \varepsilon_{yy} & 0\\ 0 & 0 & \varepsilon_{zz}\end{bmatrix},\quad \underline{\mu}=\begin{bmatrix}\mu_{xx} & \mu_{xy} & 0\\ \mu_{yx} & \mu_{yy} & 0\\ 0 & 0 & \mu_{zz}\end{bmatrix}. \tag{1}$$

We will analyze only the case of H(TE) polarization (i.e., $\mathbf{H}=H_z\hat{\mathbf{z}}$), and the similar formulation of E(TM) polarization is omitted here. The partial differential equation for H polarization is [5]

$$\varepsilon_{xx}\frac{\partial^2 H_z}{\partial x^2}+\varepsilon_{yy}\frac{\partial^2 H_z}{\partial y^2}+(\varepsilon_{yx}+\varepsilon_{xy})\frac{\partial^2 H_z}{\partial x\,\partial y}+\omega^2\mu_{zz}\gamma H_z=0\ , \tag{2a}$$

$$\gamma=\varepsilon_{xx}\varepsilon_{yy}-\varepsilon_{xy}\varepsilon_{yx}\ . \tag{2b}$$

Following Monzon and Damaskos [5], the magnetic field inside a circle can be written as

$$H_z(\rho,\varphi)=\int_0^{2\pi}c(\varphi_k)e^{jk(\varphi_k)\rho\cos(\varphi-\varphi_k)}d\varphi_k\ , \tag{3a}$$

$$k(\varphi_k)=\left[\frac{m_z^2}{\varepsilon_+ +\varepsilon_-\cos2\varphi_k+\sigma_+\sin2\varphi_k}\right]^{1/2}, \tag{3b}$$

$$m_z=\omega\sqrt{\mu_{zz}\gamma},\quad \varepsilon_\pm=\tfrac{1}{2}(\varepsilon_{xx}\pm\varepsilon_{yy}),\quad \sigma_\pm=\tfrac{1}{2}(\varepsilon_{xy}\pm\varepsilon_{yx})\ , \tag{3c}$$

where $c(\varphi_k)$ is the undetermined angular spectrum amplitude. The right-hand side of Eq. (3a) represents the exact solution of the first kind to the nonstandard Helmholtz Eq. (2a).

It is easy to see that for a given φ_k, $e^{jk(\varphi_k)\rho\cos(\varphi-\varphi_k)}$ is a solution of the first kind to the standard Helmholtz equation

$$\left[\frac{\partial^2}{\partial x^2}+\frac{\partial^2}{\partial y^2}+k^2(\varphi_k)\right]H_z^{(1)}(\rho,\varphi,\varphi_k)=0\ . \tag{4}$$

From the well known plane-wave expansion [5], it follows that

$$e^{jk(\varphi_k)\rho\cos(\varphi-\varphi_k)}=\sum_{m=-\infty}^{\infty}j^{-m}e^{-jm\varphi_k}J_m(k(\varphi_k)\rho)e^{jm\varphi}\ . \tag{5}$$

Since Eq. (4) is a homogeneous one and $\{J_m(k(\varphi_k)\rho)e^{jm\varphi}\}$ is a complete basis inside a circle $[m\epsilon(-\infty,\ldots,-2,-1,0,2,\ldots,+\infty)]$, the general solution of the first kind to Eqs. (4) and (2a) can be uniquely written as

$$H_z^{(1)}(\rho,\varphi)=\int_0^{2\pi}H_z^{(1)}(\rho,\varphi,\varphi_k)d\varphi_k \tag{6a}$$

and

$$H_z^{(1)}(\rho,\varphi,\varphi_k)=c(\varphi_k)e^{jk(\varphi_k)\rho\cos(\varphi-\varphi_k)}=c(\varphi_k)\sum_{m=-\infty}^{\infty}j^{-m}e^{-jm\varphi_k}J_m(k(\varphi_k)\rho)e^{jm\varphi}\ , \tag{6b}$$

respectively. Instead of direct verification [5], we view Eq. (6a) as an integral with a parameter variable. Therefore, the right-hand side of Eq. (6a) satisfies Eq. (4) provided that $c(\varphi_k)$ satisfies some smooth conditions. The general solution of the ith kind to Eq. (2) can be defined as

$$H_z^{(i)}(\rho,\varphi)=\int_0^{2\pi}H_z^{(i)}(\rho,\varphi,\varphi_k)d\varphi_k \ , \tag{7a}$$

$$H_z^{(i)}(\rho,\varphi,\varphi_k)=c_i(\varphi_k)\sum_{m=-\infty}^{\infty} j^{-m}e^{-jm\varphi_k}Z_m^{(i)}(k(\varphi_k)\rho)e^{jm\varphi} \ , \tag{7b}$$

$$Z_m^{(i)}(x)=\begin{cases} J_m(x), & i=1\\ Y_m(x)=[H_m^{(1)}(x)-H_m^{(2)}(x)]/(2j), & i=2\\ H_m^{(1)}(x), & i=3\\ H_m^{(2)}(x), & i=4 \ ,\end{cases} \tag{7c}$$

where $c_i(\varphi_k)$ is the undetermined angular spectrum amplitude and $Z_m^{(i)}(x)$ is the Bessel function of ith kind and mth order.

Obviously, the general solution of the ith kind as given in Eq. (7) is obtained by replacing the Bessel functions of the first kind in Eq. (6) with those of the ith kind. It can be easily shown that Eqs. (7a) and (7b) are solutions to the nonstandard wave equation (2a) and standard equation (4), respectively, since the Bessel functions of the ith kind satisfy the same equation as the Bessel functions of the first kind. It is mathematically strict that Eq. (6a) includes all solutions of the first kind since Eq. (6a) is derived by Fourier transformation [5,13]. It is also physically evident that no solution is left out since Eq. (6a) represents fields inside a circle being the superposition of eigen plane waves over all the wave-vector directions. However, some readers of Refs. [13–15] believe [21] that the simple replacement of $J_m(x)$ by $Z_m^{(i)}(x)$ may lose some solutions, then, the definition of Eq. (7) and the series solutions of wave functions are all questionable. In particular, they do not understand why the integral interval of the integration with respect to φ_k in the representation of the general solution and wave functions of the ith kind is the same interval $[0,2\pi]$ as in Eqs. (3a) and (6a). In the following, we shall resolve the doubt.

It is well known that any solution of the ith kind to the standard Helmholtz Eq. (4) can be expanded by $\{Z_m^{(i)}(k(\varphi_k)\rho)e^{jm\varphi}\}$ [17,22–24] as follows:

$$H_z^{(i)}(\rho,\varphi,\varphi_k)=\sum_{m=-\infty}^{\infty} a_m Z_m^{(i)}(k(\varphi_k)\rho)e^{jm\varphi} \ . \tag{8}$$

Replacing $Z_m^{(i)}(k(\varphi_k)\rho)$ with $J_m(k(\varphi_k)\rho)$ in Eq. (8), we get *one* solution of the first kind to Eq. (4) [13,17,22–24]. Because $c(\varphi_k)$ represents an arbitrary constant and $\{J_m(k(\varphi_k)\rho)e^{jm\varphi}\}$ is a complete basis inside a circle, we have

$$H_z^{(1)}(\rho,\varphi,\varphi_k)=\sum_{m=-\infty}^{+\infty} a_m J_m(k(\varphi_k)\rho)e^{jm\varphi}=c(\varphi_k)c_{i0}(\varphi_k)\sum_{m=-\infty}^{+\infty} j^{-m}e^{-jm\varphi_k}\times J_m(k(\varphi_k)\rho)e^{jm\varphi} \ , \tag{9a}$$

$$a_m=c(\varphi_k)c_{i0}(\varphi_k)j^{-m}e^{-jm\varphi_k} \ , \tag{9b}$$

where $c_{i0}(\varphi_k)$ is due to the homogeneity of Eq. (4). Equation (9) implies that there is one to one mapping between $H_z^{(1)}(\rho,\varphi,\varphi_k)$ and $H_z^{(i)}(\rho,\varphi,\varphi_k)$ in the sense of different coefficient $c_{i0}(\varphi_k)$. So, the integral intervals of the integration in the general solution of various kinds must be $[0,2\pi]$. Let $c_i(\varphi_k)=c(\varphi_k)c_{i0}(\varphi_k)$, we show that *any* solution of the ith kind to Eq. (4) can be written as Eq. (7b). Therefore, Eq. (7b) actually represents *all* solutions of the ith kind to Eq. (4), and Eq. (7a) represents the general solution of the ith kind to Eq. (2).

Now, the field in an annular region can be written as

$$H_z(\rho,\varphi)=\int_0^{2\pi}c_1(\varphi_k)\sum_{m=-\infty}^{+\infty} j^{-m}e^{-jm\varphi_k}J_m(k(\varphi_k)\rho)e^{jm\varphi}d\varphi_k+\int_0^{2\pi}c_2(\varphi_k)\sum_{m=-\infty}^{+\infty} j^{-m}e^{-jm\varphi_k}Y_m(k(\varphi_k)\rho)e^{jm\varphi}d\varphi_k \ , \tag{10a}$$

or equivalently

$$H_z(\rho,\varphi)=\int_0^{2\pi}c_3(\varphi_k)\sum_{m=-\infty}^{+\infty} j^{-m}e^{-jm\varphi_k}H_m^{(1)}(k(\varphi_k)\rho)e^{jm\varphi}d\varphi_k+\int_0^{2\pi}c_4(\varphi_k)\sum_{m=-\infty}^{+\infty} j^{-m}e^{-jm\varphi_k}H_m^{(2)}(k(\varphi_k)\rho)e^{jm\varphi}d\varphi_k \ . \tag{10b}$$

The outgoing waves in the homogeneous anisotropic media can be written as $[\exp(j\omega t)]$

$$H_z(\rho,\varphi)=\int_0^{2\pi}c_4(\varphi_k)\sum_{m=-\infty}^{+\infty} j^{-m}e^{-jm\varphi_k}H_m^{(2)}(k(\varphi_k)\rho)e^{jm\varphi}d\varphi_k \ . \tag{11}$$

Expanding $c_i(\varphi_k)$ in terms of the complete set $\{e^{jm\varphi_k}\}$, we have

$$c_i(\varphi_k)=\sum_{n=-\infty}^{+\infty} a_n^i e^{jn\varphi_k} \tag{12}$$

and

$$H_z^{(i)}(\rho,\varphi)=\sum_{n=-\infty}^{+\infty} a_n^i H_{zn}^{(i)}(\rho,\varphi) , \quad (13a)$$

$$H_{zn}^{(i)}(\rho,\varphi)=\sum_{m=-\infty}^{\infty} H_{znm}^{(i)}(\rho)e^{jm\varphi} , \quad (13b)$$

with

$$H_{znm}^{(i)}(\rho)=\int_0^{2\pi} j^{-m}e^{j(n-m)\varphi_k} Z_m^{(i)}(k(\varphi_k)\rho)d\varphi_k , \quad (13c)$$

where $H_{zn}^{(i)}(\rho,\varphi)$ is the wave function of the ith kind for the anisotropic media. It should be noted that the above analysis can be easily extended to the three-dimensional cylindrical and spherical cases, and for this reason, the fields are defined directly as the wave functions for anisotropic media while the wave functions for isotropic media are defined by the generating scalar functions [17]. It is also interesting that there are similarities between the scalar circular wave functions in anisotropic media and the circular-cylindrical-wave-function series representation of elliptic cylindrical wave functions in isotropic media. The fields in an anisotropic medium can be expanded by these wave functions as follows:

$$H_z(\rho,\varphi)=\sum_i \sum_{n=-\infty}^{\infty} a_n^i H_{zn}^{(i)}(\rho,\varphi) . \quad (14a)$$

The convergence of the expansion (14a) for $H_z(\rho,\varphi)$ and similar expansions for the partial derivatives of the first order of $H_z(\rho,\varphi)$ are guaranteed by the smooth property of $c_i(\varphi_k)$ [17], the completeness of the set $\{e^{jn\varphi_k}\}$, and the energy finite condition of all the components of electromagnetic fields. In fact, for any $\varepsilon>0$, there exist integer $N_i>0$, such that $n>N_i$ implies that

$$\left| c_i(\varphi_k)-\sum_{n=-\infty}^{\infty} a_n^i e^{jn\varphi_k} \right| <\varepsilon . \quad (14b)$$

Noting that for the admissable solutions of given (ρ,φ), we always truncate the (convergent for $i=1$, and asymptotic for $i=2,3,4$) series $\sum_{m=-\infty}^{+\infty} j^{-m}e^{-jn\varphi_k} Z_m^{(i)}((\varphi_k)\rho)e^{jn\phi}$ as a finite summation, and so we have

$$\left| \sum_{m=-M}^{M} j^{-m}e^{-jm\varphi_k} Z_m^{(i)}(k(\varphi_k)\rho)e^{jm\varphi} \right| \le M_i , \quad (14c)$$

where M_i is independent of φ_k. Then,

$$\left| \int_0^{2\pi} c_i(\varphi_k) \left[\sum_{m=-M}^{+M} j^{-m}e^{-jm\varphi_k} Z_m^{(i)}(k(\varphi_k)\rho)e^{jm\varphi} \right] d\varphi_k - \int_0^{2\pi} \sum_{n=-\infty}^{+\infty} a_n^i e^{jn\varphi_k} \left[\sum_{m=-M}^{+M} j^{-m}e^{-jm\varphi_k} Z_m^{(i)}(k(\varphi_k)\rho)e^{jm\varphi} \right] d\varphi_k \right| \le 4\pi^2 M_i \varepsilon . \quad (14d)$$

This shows that the solution of the series of wave functions is convergent, and the asymptotic property [22] of $\sum_{m=-\infty}^{+\infty} j^{-m}e^{-jm\varphi_k} Z_m^{(i)}(k(\varphi_k)\rho)e^{jm\varphi} (i=2,3,4)$ does not affect the convergence of the solution series of wave functions since both the general solution and each wave function contain the asymptotic series.

Quite similar to the elliptic cylindrical wave functions [17,19,20], the wave functions of the first, second, third, and fourth kind for anisotropic media represent the inward standing waves, outward standing waves, incoming waves, and outgoing waves, respectively. Therefore, the fields inside a circle can be expanded in terms of a series of wave functions of the first kind; the scattered fields outside a circle can be expanded by a series of wave functions of the fourth kind; and the fields in an annular region can be expanded by two series of the wave functions of the third and the fourth kind or the first and second kind. So, for the scattering from an anisotropic coated circular cylinder discussed in this paper, the fields in the region $a<\rho<b$ can be written as

$$H_z(\rho,\varphi)=\sum_{n=-\infty}^{\infty} j^{-n}e^{jn\varphi} \sum_{K=-\infty}^{\infty} [H_{nK}^{(1)}(\rho)a_K+H_{nK}^{(2)}(\rho)b_K] , \quad (15a)$$

$$E_\varphi(\rho,\varphi)=\sum_{n=-\infty}^{\infty} j^{-n}e^{jn\varphi} \times \sum_{K=-\infty}^{\infty} [E_{nK}^{(1)}(\rho)a_K+E_{nK}^{(2)}(\rho)b_K] , \quad (15b)$$

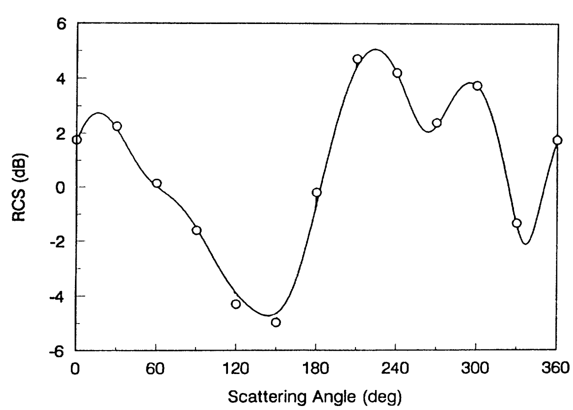

FIG. 2. H polarization, bistatic radar cross sections RCS σ/λ dB, $\varepsilon_{xx}=1.5\varepsilon_0$, $\varepsilon_{yy}=2.5\varepsilon_0$, $\varepsilon_{xy}=-\varepsilon_{yx}=3\varepsilon_0$, $\mu_{zz}=1.5\mu_0$, $\varphi^{inc}=180°$, $ka=1$, and $kb=2$. The markers are the solution taken from Ref. [9] [Fig. 9(c)].

TABLE I. Bistatic radar cross sections RCS (dB) of TE case for the structure depicted in Fig. 1: $\varepsilon_{xx}=1.5\varepsilon_0$, $\varepsilon_{yy}=2.5\varepsilon_0$, $\varepsilon_{xy}=-\varepsilon_{yx}=3\varepsilon_0$, $\mu_{zz}=1.5\mu_0$, $\varphi^{\text{inc}}=180°$, and $ka=0.5kb$.

RCS	$kb=2$		$kb=6$		$kb=8$		$kb=10$	
$\varphi°$	$N=7$	$N=12$	$N=17$	$N=20$	$N=21$	$N=25$	$N=26$	$N=30$
0	1.676 329	1.676 846	12.172 88	12.172 88	14.748 05	14.748 25	16.949 75	16.949 79
30	2.147 827	2.148 334	−4.309 279	−4.309 382	2.385 602	2.3851 03	14.792 82	14.789 21
60	8.762E-03	8.923E-03	−4.752 508	−4.752 851	−2.551 327	−2.550 842	−1.715 268	−1.736 505
90	−1.536 383	−1.536 683	0.104 206 4	0.103 638 3	10.831 51	10.832 83	15.310 05	15.311 28
120	−3.896 150	−3.896 802	3.648 235	3.648 544	6.535 048	6.534 135	11.499 37	11.496 46
150	−4.648 539	−4.648 144	−0.572 012 1	−0.572 208 2	−10.665 74	10.665 71	7.779 786	7.777 493
180	−0.634 626 4	−0.631 135	6.847 703	6.847 756	9.266 522	9.266 107	16.235 64	16.235 69
210	4.434 121	4.434 342	3.665 433	3.665 240	8.496 802	8.496 401	17.973 35	17.975 51
240	4.176 788	4.176 693	12.299 26	12.299 20	13.441 75	13.441 83	5.375 122	5.393 405
270	2.278 551	2.278 494	11.460 29	11.460 42	17.540 84	17.540 85	−2.677 653	−2.629 369
300	3.733 85	3.733 701	7.315 776	7.3158 24	17.498 02	17.497 77	3.951 855	3.946 030
330	−1.422 649	−1.422 797	3.100 958	3.100 924	14.477 01	14.476 92	7.273 975	7.275 136
360	1.676 331	1.6768 47	12.172 88	12.172 88	14.748 05	14.748 25	16.949 76	16.949 79

where

$$H_{nK}^{(1)}(\rho)=\int_0^{2\pi} J_n(k(\varphi_k)\rho)e^{j(K-n)\varphi_k}d\varphi_k \ , \qquad (16a)$$

$$H_{nK}^{(2)}(\rho)=\int_0^{2\pi} Y_n(k(\varphi_k)\rho)e^{j(K-n)\varphi_k}d\varphi_k \ , \qquad (16b)$$

$$E_{nK}^{(1)}(\rho)=-\int_0^{2\pi}\frac{k(\varphi_k)}{\omega\gamma}\left\{-j\varepsilon_{\rho\rho}(\varphi_k)J_n'(k(\varphi_k)\rho)\ , +\frac{n}{k(\varphi_k)\rho}J_n(k(\varphi_k)\rho)\times\varepsilon_{\varphi\rho}\left[\varphi_k+\frac{\pi}{2}\right]\right\}\times e^{j(K-n)\varphi_k}d\varphi_k \ , \qquad (16c)$$

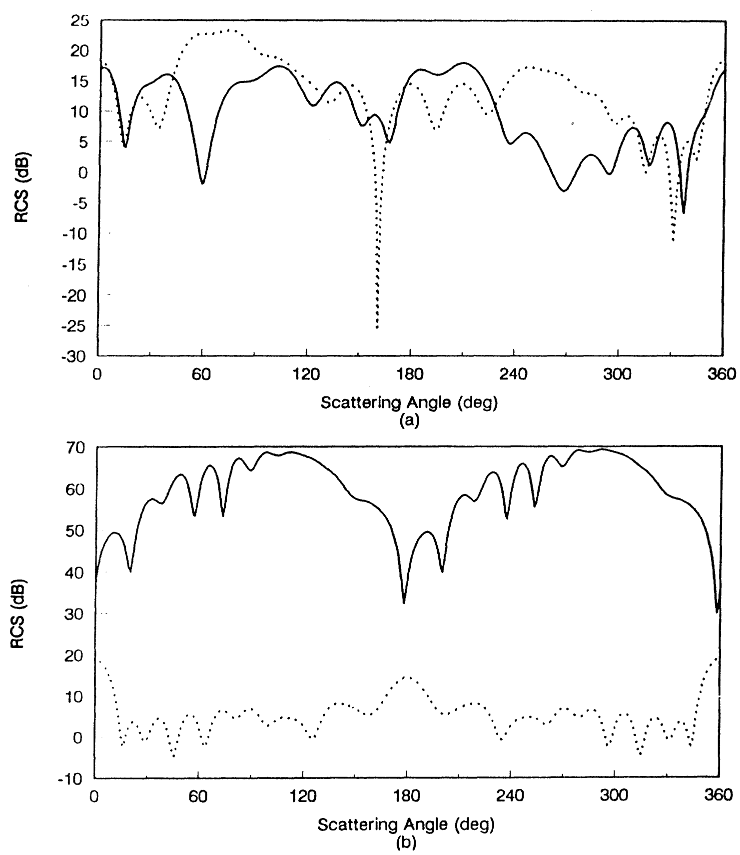

FIG. 3. H polarization bistatic RCS σ/λ dB, $\varphi^{\text{inc}}=180°$, $kb=10$, $ka=5$ (solid line), $ka=7.5$ (dotted line). (a) $\varepsilon_{xx}=1.5\varepsilon_0$, $\varepsilon_{yy}=2.5\varepsilon_0$, $\varepsilon_{xy}=-\varepsilon_{yz}=3\varepsilon_0$, and $\mu_{zz}=1.5\mu_0$. (b) $\varepsilon_{xx}=\varepsilon_0$, $\varepsilon_{yy}=4\varepsilon_0$, $\varepsilon_{xy}=\varepsilon_{yx}=0$, and $\mu_{zz}=2\mu_0$.

$$E_{nK}^{(2)}(\rho)=-\int_0^{2\pi}\frac{k(\varphi_k)}{\omega\gamma}\left\{-j\varepsilon_{\rho\rho}(\varphi_k)Y_n'(k(\varphi_k)\rho)+\frac{n}{k(\varphi_k)\rho}Y_n(k(\varphi_k)\rho)\times\varepsilon_{\varphi\rho}\left[\varphi_k+\frac{\pi}{2}\right]\right\}\times e^{j(K-n)\varphi_k}d\varphi_k\ , \tag{16d}$$

and

$$\varepsilon_{\rho\rho}(\varphi_k)=\varepsilon_+ + \varepsilon_-\cos 2\varphi_k+\sigma_+\sin 2\varphi_k\ , \tag{17a}$$

$$\varepsilon_{\varphi\rho}(\varphi_k)=-\sigma_- + \sigma_+\cos 2\varphi_k-\varepsilon_-\sin 2\varphi_k\ . \tag{17b}$$

Outside the anisotropic coated circular cylinder (i.e., in the region $\rho>b$), the incident fields (designated by the superscript inc) and scattering fields (designated by the superscript s) are expanded as

$$H_z^{\rm inc}=\sum_{n=-\infty}^{\infty} j^{-n}J_n(k\rho)e^{jn\varphi}e^{-jn\varphi^{\rm inc}}\ , \tag{18a}$$

$$E_\varphi^{\rm inc}=\sum_{n=-\infty}^{\infty} j^{-n+1}J_n'(k\rho)\left[\frac{\mu_0}{\varepsilon_0}\right]^{1/2}e^{jn\varphi}e^{-jn\varphi^{\rm inc}}\ , \tag{18b}$$

$$H_z^s=\sum_{n=-\infty}^{\infty} j^{-n}G_nH_n^{(2)}(k\rho)e^{jn\varphi}\ , \tag{18c}$$

$$E_\varphi^s=\sum_{n=-\infty}^{\infty} j^{-n+1}G_nH_n^{(2)}(k\rho)\left[\frac{\mu_0}{\varepsilon_0}\right]^{1/2}e^{jn\varphi}\ . \tag{18d}$$

The boundary conditions at $\rho=a$ and $\rho=b$ lead to three linear systems of equations, from which we obtain a_K, b_K, and

$$G_n=\frac{1}{H_n^{(2)}(kb)}\sum_{K=-\infty}^{\infty}[H_{nK}^{(1)}(b)a_K+H_{nK}^{(2)}(b)b_K]-J_n(kb)e^{-jn\varphi^{\rm inc}}\ , \tag{19}$$

as well as the bistatic radar cross sections [5]

$$\frac{\sigma}{\lambda}(\varphi,\varphi^{\rm inc})=\frac{2}{\pi}\left|\sum_{-N}^{N}(-1)^nG_ne^{jn\varphi}\right|^2\ , \tag{20}$$

where all the quantities in Eq. (20) are shown in Fig. 1.

III. NUMERICAL RESULTS

In our formulation given in Sec. II, there is no integral equation to be solved. All the integrals appearing in the matrix elements of the linear system of equations can be accurately calculated by an efficient quadrature. With this powerful quadrature, the integrals monotonically converge and remain unchanged when the node number increases to about $4N$ [for N see Eq. (20)], which is a relatively small number. Our results are checked against results available from Ref. [9] where an integral equation solver was used. Each curve presented in this paper is produced in terms of 360 data.

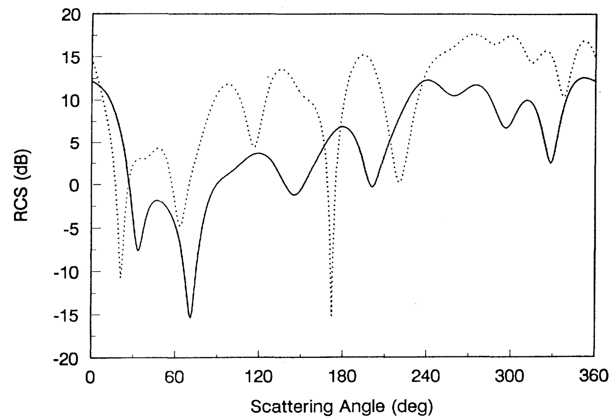

FIG. 4. H polarization, bistatic RCS σ/λ (dB), $\varphi^{\rm inc}=180°$, $a=0.5b$, $kb=6$ (solid line), $kb=8$ (dotted line), $\varepsilon_{xx}=1.5\varepsilon_0$, $\varepsilon_{yy}=2.5\varepsilon_0$, $\varepsilon_{xy}=-\varepsilon_{yx}=3\varepsilon_0$, and $\mu_{zx}=1.5\mu_0$.

We present in Fig. 2 the bistatic radar cross sections (RCS) of the anisotropic-coated conducting cylinder for the TE case of $\varphi^{\rm inc}=180°$. For the sake of comparison, the geometry and material parameters are the same as those of Fig. 9(c) of Ref. [9], i.e., $\varepsilon_{xx}=1.5\varepsilon_0$, $\varepsilon_{yy}=2.5\varepsilon_0$, $\varepsilon_{xy}=-\varepsilon_{yx}=3\varepsilon_0$, $\mu_{zz}=1.5\mu_0$, $ka=1$, and $kb=2$. It should be mentioned that a and b in our notation are two times those in Ref. [9]. Both this paper's results (solid line) and those of Beker, Umashankar, and Taflove [markers which are read from Fig. 9(c) of Ref. [9]] are displayed in Fig. 2. It can be seen that the agreement is excellent. For the purpose of further comparison and reference with other methods by other authors, we also present Table I, in which the RCS of different electrical size with the same medium parameters as those in Fig. 2 are presented. In Table I, we also show the numerical results with different N, which relate to the matrix size of the calculation. It is evident from this table that between

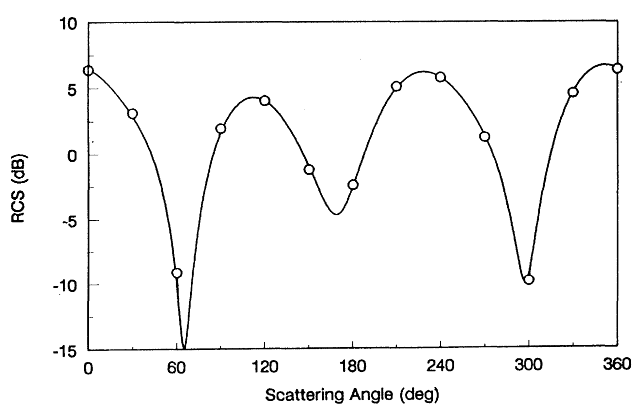

FIG. 5. E polarization, bistatic RCS σ/λ (dB), $\varphi^{\rm inc}=180°$, $\mu_{xx}=1.5\mu_0$, $\mu_{yy}=2.5\mu_0$, $\mu_{xy}=-\mu_{yx}=3\mu_0$, $\varepsilon_{zz}=1.5\varepsilon_0$, $ka=1$, and $kb=2$. The markers are the solution taken from Ref. [9] [Fig. 6(c)].

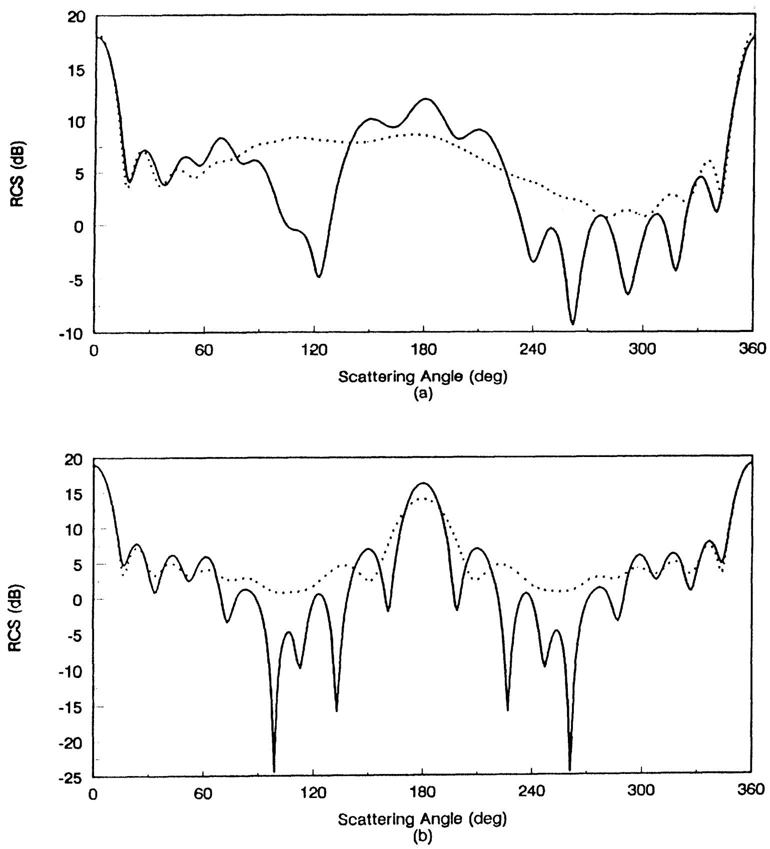

FIG. 6. E polarization, bistatic RCS σ/λ (dB), $\varphi^{\mathrm{inc}}=180°$, $kb=10$, $ka=5$ (solid line), and $ka=7.5$ (dotted line). (a) $\mu_{xx}=1.5\mu_0$, $\mu_{yy}=2.5\mu_0$, $\mu_{xy}=-\mu_{yx}=3\mu_0$, and $\varepsilon_{zz}=1.5\varepsilon_0$. (b) $\mu_{xx}=\mu_0$, $\mu_{yy}=4\mu_0$, $\mu_{xy}=\mu_{yx}=0$, and $\varepsilon_{zz}=2\varepsilon_0$.

these two N values, the results are stable. Also, as shown in Table I, the matrix size of our method is much smaller than that of Refs. [8,9]. For example, when $kb=10$, the predicted matrix size of Ref. [9] will be about 5000×5000 (as reported by Beker, Umashankar, and Taflove in Ref. [9], for $ks=10$, the matrix size is 592×592, the present ks is $10\times2\pi+5\times2\pi=94.248$, then the matrix size is about 5579×5579), while our matrix size is 61×61 only. Therefore, the high efficiency of the wave-function solution to an anisotropic-coated circular cylinder is clearly shown.

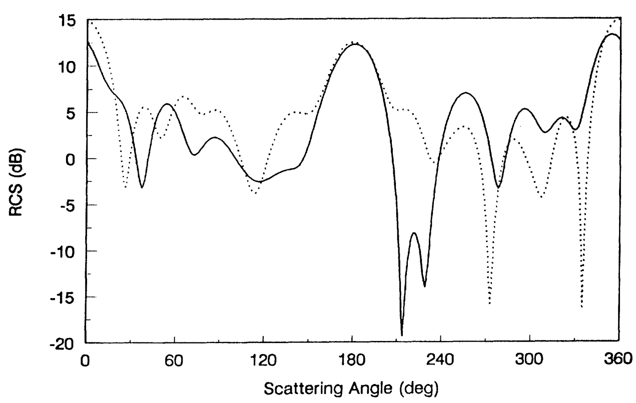

FIG. 7. E polarization, bistatic RCS σ/λ (dB), $\varphi^{\mathrm{inc}}=180°$, $a=0.5b$, $kb=6$ (solid line), $kb=8$ (dotted line), $\mu_{xx}=1.5\mu_0$, $\mu_{yy}=2.5\mu_0$, $\mu_{xy}=-\mu_{yx}=3\mu_0$, and $\varepsilon_{zz}=1.5\varepsilon_0$.

Due to the relatively few published scattering data, we presented the TE case RCS of an anisotropic-coated conducting circular cylinder versus different coating thickness and medium parameters in Fig. 3. Two cases of different thicknesses are considered. In the first case (solid line) $a=\frac{1}{2}b$, and in the second (dotted line) $a=\frac{3}{4}b$. In Fig. 3(a), $\varphi^{\mathrm{inc}}=180°$, $\varepsilon_{xx}=1.5\varepsilon_0$, $\varepsilon_{yy}=2.5\varepsilon_0$, $\varepsilon_{xy}=-\varepsilon_{yx}=3\varepsilon_0$, $\mu_{zz}=1.5\mu_0$, $kb=10$, and in Fig. 3(b), $\varphi^{\mathrm{inc}}=180°$, $\varepsilon_{xx}=\varepsilon_0$, $\varepsilon_{yy}=4\varepsilon_0$, $\varepsilon_{xy}=\varepsilon_{yx}=0$, $\mu_{zz}=2\mu_0$, $kb=10$. It can be seen from Fig. 3 that the medium parameters greatly affect the RCS of the same geometry; and the oscillation becomes fast as the coated thickness decreases for identical kb, which is expected since a conducting cylinder is a strong scattering target, and then the reaction of the conducting cylinder will be stronger as the coating thickness become thinner.

Figure 4 shows the effects of different electrical size for the same medium parameters as those of Fig. 2, and the same ratio of b/a, for $kb=6$ (solid line) and $kb=8$ (dotted line), respectively. As expected, with an increasing electrical size the oscillation is indeed more rapid.

To illustrate applicability of the wave-function solution to the TM case of scattering by an anisotropic-coated circular conducting cylinder, the RCS are claculated for the TM case. Figures 5, 6, and 7 for the TM case correspond to Figs. 2, 3, and 4 for the TE case, respectively. For example, the material parameters and electrical size of Figs. 5, 6, and 7 for the TM case are the same as those of Figs. 2, 3, and 4 for the TE case, respectively; the markers in Fig. 5 represent the numerical results given in Fig. 6(c) of

Ref. [9]. Similar conclusions to the TE case can be drawn from these figures for the TM case.

It should be indicated that the CPU time for all calculations shown in this paper is less than 8 min in VAX-6510.

IV. DISCUSSION AND CONCLUSION

Equations (7a) and (7b) have clearly physical meaning in their own right. It implies that the fields in homogeneous anisotropic media can be viewed as the superposition of fields in all the eigenwave vector directions. In each eigenvwave vector direction, the field satisfies the standard wave equation in isotropic media. Furthermore, Eqs. (7a) and (7b) give the mathematical structure [25] of the general solutions to Eq. (2). The general solution of the ith kind to the nonstandard wave equation (2) can be constructed by an integral over φ_k in the interval $[0,2\pi]$ and the integrand being the solution to the standard Eq. (4). Each solution of the ith kind to Eq. (4) is obtained by a simple replacement of $Z_m^{(i)}(x)$ with $J_m(x)$ in the solution of the first kind, which is easily derived by expanding the plane-wave factor. Such a procedure transforms the eigen plane-wave theory in unbounded space into the general solutions suitable for bounded geometries, which is the common foundation of wave-function theories [13–15,26,27] in homogeneous anisotropic media. The above mathematical interpretation is useful in understanding the introduction of Eq. (4) and the physical mechanism of waves in bounded homogeneous anisotropic media. For example, such a physical mechanism is quite useful in the study of dipole radiation in unbounded anisotropic media [26]. The clearly mathematical structure of the general solutions to the wave equation in anisotropic media suggests an alternative wave-function theory based on spline approximation of the undetermined angular spectrum amplitude [27]. In the alternative theory, each wave function is an integral with respect to partial eigenwaves due to the compact property of splines instead of all eigenwaves [5]. Only the general solution (a summation of alternative wave functions) must include the contributions of all eigenwaves. Moreover, the mathematical structure of the general solutions suggests the direct discretization of the integral representation of general solutions [27]. The details of such discretization is discussed in a separate article [28].

In conclusion, Ren's solution to the homogeneous wave equations in anisotropic media is correct. The convergence of the wave-function series are proven. The theory presented in this paper can be easily extended to cover any wave equations in homogeneous anisotropic media in which the eigen plane-wave solution is available. This paper's theory can be generalized to the general solution, series solution, and fundamental solution (Green's function) of the n-dimensional $(n>3)$ wave equations with constant coefficients [29]. And this is important in some mathematical physics applications. Numerical computations show the very high computational efficiency of the series solution for circular geometries. Moreover, our calculations show that the theoretical work [13] on the open problem about the fields in an annular region is correct, and the wave-function solution is powerful and worthwhile for further study. We should reecognize that this article is only a preliminary application work. Finally, the main advantage of the series solution is its easy extension to three-dimensional cylindrically and spherically layered structures [13–15]. Moreover, after the use of a recursive algorithm the computational efficiency of the wave-function solution is more clearly shown when more than one coating layer is present [30].

ACKNOWLEDGMENTS

W.R. is greatly indebted to Dr. B. Beker for sending us his data. This work was supported by the National Natural Science Foundation of China.

[1] R. D. Graglia and P. L. E. Uslenghi, Electromagnetics **7**, 117 (1987).
[2] H. Massoudi, N. J. Damaskos, and P. L. E. Uslenghi, Electromagnetics **8**, 71 (1988).
[3] R. D. Graglia, P. L. E. Uslenghi, and R. S. Zich, Proc. IEEE **77**, 750 (1989).
[4] R. B. Wu and C. H. Chen, IEEE Trans. Antennas Propagat. **34**, 640 (1986).
[5] J. C. Monzon and N. J. Damaskos, IEEE Trans. Antennas Propag. **34**, 1243 (1986).
[6] J. C. Monzon, IEEE Trans. Antennas Propag. **35**, 670 (1987).
[7] J. C. Monzon, IEEE Trans. Antennas Propag. **36**, 1401 (1988).
[8] B. Beker, K. R. Umashankar, and A. Taflove, IEEE Trans. Antennas Propag. **37**, 1573 (1989).
[9] B. Beker, B. K. R. Umashankar, and A. Taflove, Electromagnetics **10**, 387 (1990).
[10] V. V. Varadan, A. Lakhtakia, and V. K. Varadan, IEEE Trans. Antennas Propag. **37**, 800 (1989).
[11] S. N. Papadakis, N. Uzunoglu, and C. N. Capsalis, J. Opt. Soc. Am. A **7**, 991 (1990).
[12] C. M. Rappaport and B. J. McCartin, IEEE Trans. Antennas Propag. **39**, 345 (1991).
[13] W. Ren, Phys. Rev. E **47**, 664 (1993); **47**, 4439 (1993).
[14] W. Ren, J. Acoust. Soc. Am. **95**, 1741 (1994).
[15] W. Ren, J. Math. Phys. **34**, 5376 (1993).
[16] R. D. Graglia, P. L. E. Uslenghi, and R. E. Zich, IEEE Trans. Antennas Propag. **39**, 83 (1991).
[17] J. A. Stratton, *Electromagnetic Theory* (McGraw-Hill, New York, 1941).
[18] X. B. Wu and W. Ren, Micro. Opt. Tech. Lett. (to be published).
[19] J. H. Richmond, Radio Sci. **23**, 1061 (1988).
[20] J. H. Richmond, IEEE Trans. Antennas Propag. **37**, 1235 (1989).
[21] Weiner S. Weiglhofer (unpublished).
[22] P. M. Morse and H. Feshback, *Methods of Theoretical Physics* (McGraw-Hill, New York, 1953), pp. 1411 and 1507.
[23] C. Flammer, *Spheroidal Wave Functions* (Stanford University Press, Stanford, 1957), p. 32.
[24] A. Bostrom, G. Kristenssion, and S. Strom, in *Field Representation and Introduction to Scattering,* edited by V. V.

Varadan, A. Lakhatakia, and V. K. Varadan (Elsevier, New York, 1991), Chap. 4.
[25] J. Glimm and A. Jaffe, *Quantum Physics: A Functional Integral Point of View,* 2nd ed. (Springer-Verlag, New York, 1987).
[26] W. Ren (unpublished).
[27] W. Ren and X. B. Wu, Phys. Rev. E **49**, 3528 (1994).
[28] W. Ren and X. B. Wu, J. Phys. D (to be published).
[29] W. Ren (unpublished).
[30] X. B. Wu and W. Ren (unpublished).